IOSR Journal of Mechanical and Civil Engineering (IOSR-JMCE)
e-ISSN: 2278-1684,p-ISSN: 2320-334X, Volume 18, Issue 3 Ser. III (May − June 2021), PP 10-22
www.iosrjournals.org

Buckling Solution of a Three-Dimensional Clamped Rectangular Thick Plate Using Direct Variational Method

Onyeka, F. C[1*]
[1] *Department of Civil Engineering, Edo State University Uzairue, Edo State, Nigeria.*
Okafor, F. O[2]
[2]*Department of Civil Engineering, University of Nigeria Nsukka, Nigeria.*
Onah H, N[3]
[3] *Department of Civil Engineering, University of Nigeria Nsukka, Nigeria*

Abstract
This work deals with buckling analysis of a three dimensional isotropic thick plate clamped in all the edges (CCCC) subjected to a uniaxial compressive load, using the variational Energy method. Total potential energy equation of a thick plate was formulated from the three-dimensional constitutive relations, thereafter the compatibility equations was established to obtain the relations between the deflection and shear deformation rotation along the direction of x and y coordinates. By minimizing the potential energy equation with respect to the coefficient deflection and shear deformation rotation, the formulae for calculating the critical buckling load is obtained. Using a mathematical modelling technique based on polynomial displacement function obtained from the compatibility governing equation, a buckling solution was obtained by applying the boundary conditions of the plate and substituted on buckling equation derived. From the numerical analysis obtained, it is found that the value of the critical buckling load increase as the span- thickness ratio increases. This means that an increase in plate thickness improves structural the safety of the plate. The proposed solution were validated and compared with the solution of the trigonometric function using the same model as developed. The critical buckling load was comparable for both functions at varying aspect ratio and the total average percentage difference obtained is 4.3%. The difference being close proved high convergence and accuracy of the approach in the thick plate analysis.

***Keywords**: CCCC plate, polynomial and trigonometric function, variational energy method, buckling of three-dimensional plate*

Date of Submission: 05-06-2021 Date of Acceptance: 18-06-2021

I. Introduction

Plates are three dimensional structural members and its use is on the increase in the recent years due to its economic and structural benefits such as light weight and its ability to withstand heavy loads, affordability and versatility in its applications. They are used as bridge deck, aircraft wing panel, aerospace panels and slab building structure [1-3].

Plates can be subjected to in-plane loads and transverse loads, and can be simply supported, clamped or free at the edges. The plate problem belongs to elasticity theory and is normally applied to determine the distribution of stress fields in a given plate under known loading and support conditions [4].

In avoidance of rigorous process in solving 3-D plate problems, several theories (classical plate theory (CPT), Mindlin theory and refined plate theory (RPT)) have been employed to reduce three dimensional problems to two dimensional (2-D) by integrating out the plates thickness dimension by making a kinematic assumption that the strains can be expanded in the smallest dimension [5, 6]. This assumption has discovered to have introduced errors, hence does not offer a very accurate analysis of plates in which the thickness-to-length proportion is relatively large [7, 8]. Hence, the analysis of 3-D thick plate structures is very essential. A number of theories and approaches have been suggested in the literature for the prediction of the critical buckling load of plates.

The authors in [9] used the virtual work principle for the buckling analysis of simply supported stiffened rectangular isotropic plate. They developed numerical model based on polynomial shape function which enable them to determine the buckling coefficients for a stiffened rectangular plate. They found out that their approach can be used to predict the buckling load of thin plates. The authors in [10] also adopted the approach and shape function applied to uni-axially compressed plate elastically restrained in all directions. The author in [9] did not consider CCCC boundary condition. Both authors did not consider a thick plate as their assumption is limited to the classical plate theory which will not yield a good result when the plate is relatively thick.

The authors in [11] used the different boundary condition to study the stability and vibration behavior of the elastic rectangular thick plate using the refined plate theory. The theory did not consider the stresses in the direction of thickness axis, therefore can only predict buckling load of thin and moderately thick plates. They assumed shape function, which made their result not a close-form solution and cannot be used to solve plate problems in which all edges are clamped and that heavy type of plates.

The authors in [12] simply supported boundary condition to study the buckling behavior of the elastic rectangular thick plate using the Energy approach. They found out that their approach can be used with confidence to determine the critical buckling load of plates and can be used in the analysis of thin, moderately thick, and thick plates, respectively. The authors in [12] used a derived shape function using the principle of elasticity to yield a close-form solution but they did not consider the plate with all the edge condition clamped as in this present study.

In this work, the analytical three-dimensional plate theory for isotropic plates is formulated and derived using the variational energy method, and presented as a problem of the theory of elasticity. The aim is to determine the critical buckling load of a thick rectangular plate elastically restrained along all the edges (CCCC) under uniaxial compressive load using trigonometric and polynomial displacement function derived from the governing equation. The proposed theory can be used to solve all types of plate as they consider all the stress elements in the analysis.

II. Methodology

Considering the kinematics and three-dimensional constitutive relations of a rectangular thick plate presented in the figure 1, the total potential energy of the plate is obtained through energy potential formulation.

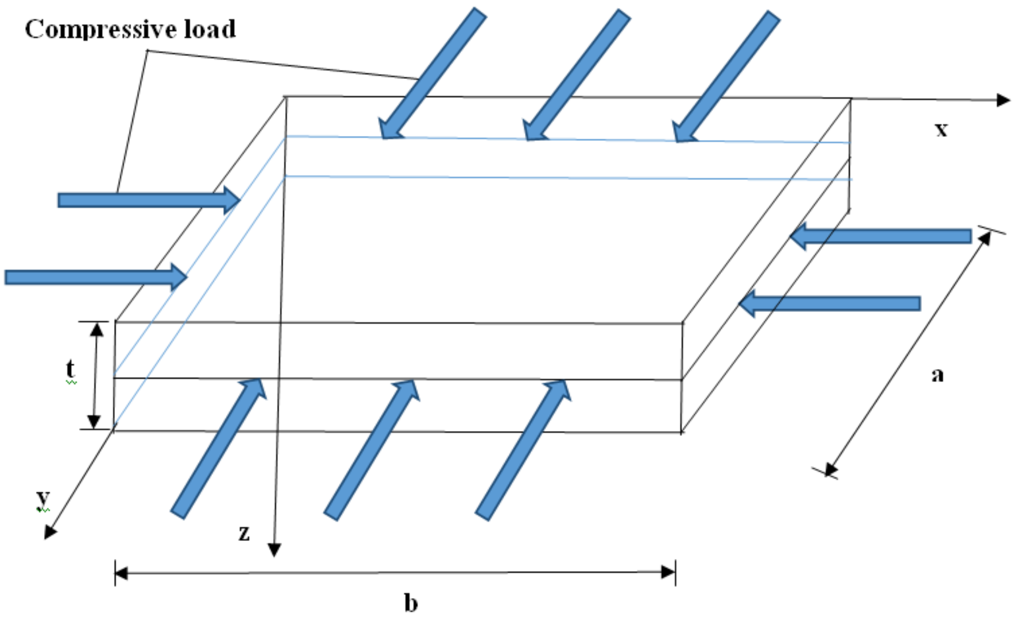

Figure 1: A rectangular thick plate element showing the in-plane compressive loading

As shown in figure 1, the spatial dimensions of the plate along x, y and z-axes are a, b and t respectively.

2.1.1. Displacement Kinematics Relations

The energy equation formulation for the stability analysis thick rectangular plate under compressive load in figure 1, will be obtained by considering its section as presented in figure 2.

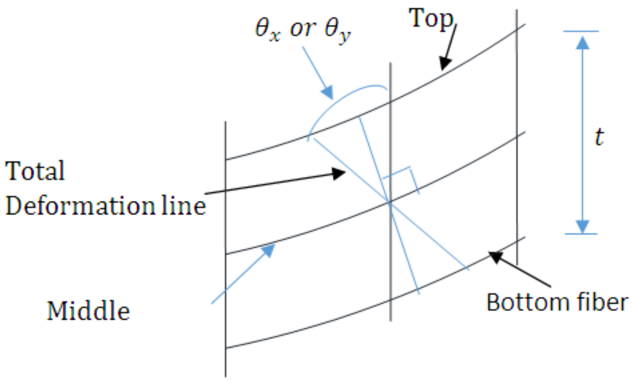

Figure 2: Rotation of x-z (or y-z) section after bending

As shown in the figure 2, the displacement field includes the displacements along x, y and z-axes: u, v and w respectively. The displacement and slope along the x axis and y axis are mathematically expressed as:

$$w = \mathrm{w(x, y)} \quad 1$$

$$\theta_x = \frac{\partial u}{\partial z} \quad 2$$

$$\theta_y = \frac{\partial v}{\partial z} \quad 3$$

Taking the non-dimensional form of coordinates to be R = x/a, Q = y/b and S = z/t corresponding to x, y and z-axes respectively,

$$\beta = b/a \quad 4$$

$$b = a\beta \quad 5$$

Also, the aspect ratio of length of the plate along x axis to the length of the plate thickness.

$$\propto = \frac{\mathrm{a}}{\mathrm{t}} \quad 6$$

Thus, the non-dimensional form of Equation 2 and 3 becomes:

$$\theta_x = \frac{1}{\mathrm{t}} \cdot \frac{\partial u}{\partial s} \quad 7$$

$$\theta_y = \frac{1}{\mathrm{t}} \cdot \frac{\partial v}{\partial s} \quad 8$$

Thus, the in-plane displacements; u and v as presented in the Equation 2 and 3 are further defined using trigonometric relations for small angles as:

$$u = z\theta_x \quad 9$$

$$v = z\theta_y \quad 10$$

Where:

The symbol w denotes deflection, the symbol u denotes in-plane displacement along x-axis, the symbol v denotes in-plane displacement along y-axis, the symbol θ_x denotes shear deformation rotation along x axis, the symbol θ_y denotes shear deformation rotation along the y axis, and z denotes shear deformation profile.

Therefore, the non-dimensional form of Equation 9 and 10 becomes:

$$u = ts.\theta_x \quad 11$$

$$v = ts.\theta_y \quad 12$$

2.1.2 Engineering Strain Components

The six strains components are ε_x, ε_y,ε_z,$\gamma_{x\text{-}y}$, $\gamma_{x\text{-}z}$, and $\gamma_{y\text{-}z}$. are defined based on the theory of elasticity as the ratios of displacement of a finite length of a plate to that of the finite length. They summarized in terms of non-dimensional as:

$$\varepsilon_x = \frac{\partial u}{a\partial R} \quad 13$$

$$\varepsilon_y = \frac{\partial v}{a\beta\partial Q} \quad 14$$

$$\varepsilon_z = \frac{\partial w}{t\partial S} \quad 15$$

$$\gamma_{xy} = \frac{\partial u}{a\beta\partial Q} + \frac{\partial v}{a\partial R} \quad 16$$

$$\gamma_{xz} = \frac{\partial u}{t\partial S} + \frac{\partial w}{a\partial R} \quad 17$$

$$\gamma_{yz} = \frac{\partial v}{t\partial S} + \frac{\partial w}{a\beta\partial Q} \quad 18$$

Substituting Equation11 into 13 gives:

$$\varepsilon_x = \frac{\text{ts}}{\text{a}} \cdot \frac{\partial \theta_x}{\partial R} \quad 19$$

Substituting Equation12 into 14 gives:

$$\varepsilon_y = \frac{ts}{\text{a}\beta} \cdot \frac{\partial \theta_y}{\partial Q} \quad 20$$

Equation15 becomes:

$$\varepsilon_z = \frac{1}{\text{t}} \cdot \frac{\partial w}{\partial s} \quad 21$$

Substituting Equations 11 and 12 into 16 gives:

$$\gamma_{xy} = \frac{\text{ts}}{\text{a}\beta} \cdot \frac{\partial \theta_x}{\partial Q} + \frac{\text{ts}}{\text{a}} \cdot \frac{\partial \theta_y}{\partial R} \quad 22$$

Substituting Equation7 into 17 gives:

$$\gamma_{xz} = \theta_x + \frac{1}{\text{a}} \cdot \frac{\partial w}{\partial R} \quad 23$$

Substituting Equation8 into 18 gives:

$$\gamma_{yz} = \theta_y + \frac{1}{\text{a}\beta} \cdot \frac{\partial w}{\partial Q} \quad 24$$

The Equations 19, 20, 21, 22, 23 and 24 are the established six strains components in the plate material.
Where:
the symbol ε_x denotes normal strain along x axis, the symbol ε_y denotes normal strain along y axis, the symbol ε_z denotes normal strain along z axis, the symbol γ_{xy} denotes shear strain in the plane parallel to the x-y plane, the symbol γ_{xz} denotes shear strain in the plane parallel to the x-z plane, the symbol γ_{yz} denotes shear strain in the plane parallel to the y-z plane.

2.1.3. Constitutive Relations

In the constitutive relation, the stresses causing the body movements are considered here. These stresses are described using generalized Hooke's law, therefore, the three dimensional constitutive relation for the isotropic material will yields the six stress components (σ_x, σ_y,σ_z, τ_{xy}, τ_{xz}, and τ_{yz}).

$$\begin{bmatrix} \sigma_x \\ \sigma_y \\ \sigma_z \\ \gamma_{xz} \\ \gamma_{yz} \\ \gamma_{xy} \end{bmatrix} = \frac{\text{E}}{(1+\mu)(1-2\mu)} \begin{bmatrix} (1-\mu) & \mu & \mu & 0 & 0 & 0 \\ \mu & (1-\mu) & \mu & 0 & 0 & 0 \\ \mu & \mu & (1-\mu) & 0 & 0 & 0 \\ 0 & 0 & 0 & \left(\frac{1\text{-}2\mu}{2}\right) & 0 & 0 \\ 0 & 0 & 0 & 0 & \left(\frac{1\text{-}2\mu}{2}\right) & 0 \\ 0 & 0 & 0 & 0 & 0 & \left(\frac{1\text{-}2\mu}{2}\right) \end{bmatrix} \begin{bmatrix} \varepsilon_x \\ \varepsilon_y \\ \varepsilon_z \\ \gamma_{xz} \\ \gamma_{yz} \\ \gamma_{xy} \end{bmatrix} \quad 25$$

Substituting Equations 19 to 24 into Equation 25 and writing the equations of the six stress components one by one in term of the displacements gives:

$$\sigma_x = \frac{\text{Ets}}{(1+\mu)(1-2\mu)\text{a}} \left[\frac{\mu}{\beta} \cdot \frac{\partial \theta_y}{\partial Q} + (1-\mu) \cdot \frac{\partial \theta_x}{\partial R} + \frac{\mu \text{a}}{st^2} \cdot \frac{\partial \text{w}}{\partial \text{S}} \right] 26$$

$$\sigma_y = \frac{\text{Ets}}{(1+\mu)(1-2\mu)\text{a}} \left[\frac{(1-\mu)}{\beta} \cdot \frac{\partial \theta_y}{\partial Q} + \mu \cdot \frac{\partial \theta_x}{\partial R} + \frac{\mu \text{a}}{st^2} \cdot \frac{\partial \text{w}}{\partial \text{S}} \right] \quad 27$$

$$\sigma_z = \frac{\text{Ets}}{(1+\mu)(1-2\mu)\text{a}} \left[\frac{(1-\mu)\text{a}}{st^2} \cdot \frac{\partial \text{w}}{\partial \text{S}} + \mu \cdot \frac{\partial \theta_x}{\partial R} + \frac{\mu}{\beta} \cdot \frac{\partial \theta_y}{\partial Q} \right] \quad 28$$

$$\tau_{xy} = \frac{1}{\beta} \frac{\partial \theta_x}{\partial Q} \cdot \frac{\text{E}(1-2\mu)ts}{2(1+\mu)(1-2\mu)\text{a}} + \frac{\text{E}(1-2\mu)ts}{2(1+\mu)(1-2\mu)\text{a}} \cdot \frac{\partial \theta_y}{\partial R} \quad 29$$

$$\tau_{xz} = \frac{\text{a}}{\text{ts}} \theta_{x.} \frac{\text{E}(1-2\mu)ts}{2(1+\mu)(1-2\mu)\text{a}} + \frac{\text{E}(1-2\mu)ts}{2(1+\mu)(1-2\mu)\text{a}} \cdot \frac{1}{\text{ts}} \frac{\partial \text{w}}{\partial \text{R}} \quad 30$$

$$\tau_{yz} = \frac{\text{a}}{\text{ts}} \theta_y \cdot \frac{\text{E}(1-2\mu)ts}{2(1+\mu)(1-2\mu)\text{a}} + \frac{\text{E}(1-2\mu)ts}{2(1+\mu)(1-2\mu)\text{a}} \cdot \frac{1}{\beta\text{ts}} \frac{\partial \text{w}}{\partial \text{Q}} \quad 31$$

Where:

E and μdenotes thePoisson's ratios and modulus of elasticity of material respectively.

2.1.4. Total Potential Energy Functional

The summation of strain energy and the external work gives the total potential energy. This mathematically expressed as:

$$\prod = \mathrm{U} - \mathrm{V} \qquad 32$$

Where:

$\prod$, V and U denotes thetotal potential energy, external works and strain energy respectively.

The strain energy being the average product of stress and strain indefinitely summed up within the spatial domain of the body.

$$\mathrm{U} = \frac{\mathrm{abt}}{2}\int_0^1\int_0^1\int_{-0.5}^{0.5}\left(\sigma_x\varepsilon_x + \sigma_y\varepsilon_y + \sigma_z\varepsilon_z + \tau_{xy}\gamma_{xy} + \tau_{xz}\gamma_{xz} + \tau_{yz}\gamma_{yz}\right)\mathrm{dR\,dQ\,dS} \qquad 33$$

However, the external work for buckling load is given as:

$$\mathrm{V} = \frac{\mathrm{abN_x}}{2\mathrm{a}^2}\int_0^a\int_0^b\left(\frac{\partial \mathrm{w}}{\partial R}\right)^2 \mathrm{dR\,dQ} \qquad 34$$

Thus, the total potential energy of the three dimensional thick rectangular plate is presented as [12]:

$$\prod = \mathrm{D}\frac{(1-\mu)ab}{2\mathrm{a}^2(1-2\mu)}\int_0^1\int_0^1\left[(1-\mu)\left(\frac{\partial\theta_{sx}}{\partial R}\right)^2 + \frac{1}{\beta}\frac{\partial\theta_{sx}}{\partial R}.\frac{\partial\theta_{sy}}{\partial Q} + \frac{(1-\mu)}{\beta^2}\left(\frac{\partial\theta_{sy}}{\partial Q}\right)^2 + \frac{(1-2\mu)}{2\beta^2}\left(\frac{\partial\theta_{sx}}{\partial Q}\right)^2 + \frac{(1-2\mu)}{2}\left(\frac{\partial\theta_{sy}}{\partial R}\right)^2 + \frac{6(1-2\mu)}{\mathrm{t}^2}\left(\mathrm{a}^2\theta_{sx}{}^2 + \mathrm{a}^2\theta_{sy}{}^2 + \left(\frac{\partial \mathrm{w}}{\partial R}\right)^2 + \frac{1}{\beta^2}\left(\frac{\partial \mathrm{w}}{\partial Q}\right)^2 + 2\mathrm{a}.\theta_{sx}\frac{\partial \mathrm{w}}{\partial R} + \frac{2\mathrm{a}.\theta_{sy}}{\beta}\frac{\partial \mathrm{w}}{\partial Q}\right) + \frac{(1-\mu)\mathrm{a}^2}{t^4}\left(\frac{\partial \mathrm{w}}{\partial S}\right)^2 - \frac{\mathrm{N_x}}{\mathrm{D}^*}.\left(\frac{\partial \mathrm{w}}{\partial R}\right)^2\right]\partial R\partial Q \qquad 35$$

Where:

$$\mathrm{D}^* = \mathrm{D}\frac{(1-\mu)}{(1-2\mu)}$$

2.1.5. Compatibility Equation

The true compatibility equations in x-z plane y-z plane according the author in [12] is obtained by minimizing the energy equation with respect to rotation in x-z plane and rotation in y-z plane and equate its integrands to zero to get:

$$(1-\mu)\frac{\partial^2\theta_{sx}}{\partial R^2} + \frac{1}{2\beta}.\frac{\partial^2\theta_{sy}}{\partial R\partial Q} + \frac{(1-2\mu)}{2\beta^2}\frac{\partial^2\theta_{sx}}{\partial Q^2} + \frac{6(1-2\mu)}{\mathrm{t}^2}\left(\mathrm{a}^2\theta_{sx} + \mathrm{a}.\frac{\partial \mathrm{w}}{\partial R}\right) = 0 \qquad 36$$

$$\frac{1}{2\beta}.\frac{\partial^2\theta_{sx}}{\partial R\partial Q} + \frac{(1-\mu)}{\beta^2}\frac{\partial^2\theta_{sy}}{\partial Q^2} + \frac{(1-2\mu)}{2}\frac{\partial^2\theta_{sy}}{\partial R^2} + \frac{6(1-2\mu)}{\mathrm{t}^2}\left(\mathrm{a}^2\theta_{sy} + \frac{\mathrm{a}.\partial \mathrm{w}}{\beta\,\partial Q}\right) = 0 \qquad 37$$

Using law of addition, the Equations 36 and 37 will be simplified, then factorizing the outcome gives:

$$\frac{\partial w}{\partial R}\left[(1-\mu)\frac{\partial^2}{\partial R^2} + \frac{1}{\beta^2}.\frac{\partial^2}{\partial Q^2}(1-\mu) + \frac{6(1-2\mu)\mathrm{a}^2}{\mathrm{t}^2}.\left(1+\frac{1}{c}\right)\right] = 0 \qquad 38$$

$$\frac{1}{\beta}.\frac{\partial \mathrm{w}}{\partial Q}\left[\frac{\partial^2}{\partial R^2}(1-\mu) + \frac{(1-\mu)}{\beta^2}\frac{\partial^2}{\partial Q^2} + \frac{6(1-2\mu)\mathrm{a}^2}{\mathrm{t}^2}.\left(1+\frac{1}{c}\right)\right] = 0 \qquad 39$$

After simplification using law of addition, one of the possible of Equation becomes:

$$\frac{6(1-2\mu)(1+c)}{\mathrm{t}^2} = -\frac{\mathrm{c}(1-\mu)}{\mathrm{a}^2}\left(\frac{\partial^2}{\partial R^2} + \frac{1}{\beta^2}\frac{\partial^2}{\partial Q^2}\right) \qquad 40$$

2.1.6. General Governing Equation

The minimization of energy equation with respect to deflection gives the general governing equation as presented in [2]:

$$\frac{\mathrm{D}^*}{2\mathrm{a}^2}\int_0^1\int_0^1\left[\frac{6(1-2\mu)(1+\mathrm{c})}{\mathrm{t}^2}\left(\frac{\partial^2\mathrm{w}}{\partial R^2} + \frac{1}{\beta^2}.\frac{\partial^2\mathrm{w}}{\partial Q^2}\right) + \frac{(1-\mu)\mathrm{a}^2}{t^4}\frac{\partial^2\mathrm{w}}{\partial S^2} - \frac{\mathrm{N_x}}{\mathrm{D}^*}.\frac{\partial^2\mathrm{w}}{\partial R^2}\right]\mathrm{dR\,dQ} = 0 \qquad 41$$

Substituting Equation 40 into Equation 41 and simplifying the outcome givestwo governing differential equations of a 3-dimensional rectangular plate subject to pure buckling as presented in Equation 42 and 43:

$$\frac{\partial^4 w_1}{\partial R^4}+\frac{2}{\beta^2}\cdot\frac{\partial^4 w_1}{\partial R^2\partial Q^2}+\frac{1}{\beta^4}\cdot\frac{\partial^4 w_1}{\partial Q^4}-\frac{N_{x1}a^4}{gD^*}\cdot\frac{\partial^2 w_1}{\partial R^2}=0 \qquad 42$$

$$\frac{(1-\mu)a^4}{t^4}\cdot\frac{\partial^2 w_S}{\partial S^2}-\frac{N_{xs}a^4}{D^*}\cdot\frac{\partial^2 w_S}{\partial R^2}=0 \qquad 43$$

Thus, the approximate solution to the differential equation of Equation 42 in polynomial form gives:

$$w=\Delta_0(a_0+\ a_1R+a_2R^2+a_3R^3+\ a_4R^4)\times(b_0+\ \ b_1Q+\ b_2Q^2+b_3Q^3+b_4Q^4) 44$$

In a more symbolized form:

$$w=A_1h \qquad 45$$

Let:

$$A_1=\Delta_0\begin{bmatrix}a_0\\a_1\\a_2\\a_3\\a_4\end{bmatrix}.\begin{bmatrix}b_0\\b_1\\b_2\\b_3\\b_4\end{bmatrix} \qquad 46$$

$$h=[1\ \ RR^2R^3R^4].[1\ \ QQ^2Q^3Q^4] \qquad 47$$

$$\theta_{sx}=\frac{A_2}{a}\cdot\frac{\partial h}{\partial R} \qquad 48$$

$$\theta_{sy}=\frac{A_3}{a\beta}\cdot\frac{\partial h}{\partial Q} \qquad 49$$

Where:

The symbol A_1 denotes coefficient of deflection, the symbol A_2 denotes coefficient of shear deformation along x axis, the symbol A_3 denotes coefficient of shear deformation along the y axis.

2.1.7. Direct Governing Equation

By differentiating the total potential energy functional with respect to deflection coefficient, the formulae for calculating the critical buckling load was obtained.

Substituting Equations (45), (48) and (49) into Equation (35) gives:

$$\Pi=\frac{D^*ab}{2a^4}\Bigg[(1-\mu){A_2}^2\int_0^1\int_0^1\left(\frac{\partial^2 h}{\partial R^2}\right)^2 dRdQ\ +\frac{1}{\beta^2}\left[A_2.A_3+\frac{(1-2\mu){A_2}^2}{2}+\frac{(1-2\mu){A_3}^2}{2}\right]\int_0^1\int_0^1\left(\frac{\partial^2 h}{\partial R\partial Q}\right)^2$$
$$+\frac{(1-\mu){A_3}^2}{\beta^4}\int_0^1\int_0^1\left(\frac{\partial^2 h}{\partial Q^2}\right)^2 dRdQ$$
$$+6(1-2\mu)\left(\frac{a}{t}\right)^2\Bigg(\left[{A_2}^2+{A_1}^2+2A_1A_2\right].\int_0^1\int_0^1\left(\frac{\partial h}{\partial R}\right)^2 dRdQ$$
$$+\frac{1}{\beta^2}.\left[{A_3}^2+{A_1}^2+2A_1A_3\right].\int_0^1\int_0^1\left(\frac{\partial h}{\partial Q}\right)^2 dRdQ\Bigg)-\frac{N_x a^2{A_1}^2}{D^*}.\int_0^1\int_0^1\left(\frac{\partial h}{\partial R}\right)^2 dRdQ\Bigg] \qquad 50$$

Differentiating Equation 50 with respect to A_2 and $A_3$and solve simultaneously gives:

$$A_2=\left(\frac{k_{12}k_{23}-k_{13}k_{22}}{k_{12}k_{12}-k_{11}k_{22}}\right).A_1 \qquad 51$$

$$A_3=\left(\frac{k_{12}k_{13}-k_{11}k_{23}}{k_{12}k_{12}-k_{11}k_{22}}\right).A_1 \qquad 52$$

Let:

$$k_{11}=(1-\mu)k_{RR}+\frac{1}{2\beta^2}(1-2\mu)k_{RQ}+6(1-2\mu)\left(\frac{a}{t}\right)^2 k_R \qquad 53$$

$$k_{21}=k_{12}=\frac{1}{2\beta^2}k_{RQ};\ k_{13}=-6(1-2\mu)\left(\frac{a}{t}\right)^2 k_R;\ k_{32}=k_{23}=-\frac{6}{\beta^2}(1-2\mu)\left(\frac{a}{t}\right)^2 k_Q \qquad 54$$

$$k_{22}=\frac{(1-\mu)}{\beta^4}k_{QQ}+\frac{1}{2\beta^2}(1-2\mu)k_{RQ}+\frac{6}{\beta^2}(1-2\mu)\left(\frac{a}{t}\right)^2 k_Q \qquad 55$$

Where:

$$k_{RR}=\int_0^1\int_0^1\left(\frac{\partial^2 h}{\partial R^2}\right)^2 dRdQ \qquad 56$$

$$k_{RQ} = \int_0^1 \int_0^1 \left(\frac{\partial^2 h}{\partial R \partial Q}\right)^2 dRdQ \qquad 57$$

$$k_{QQ} = \int_0^1 \int_0^1 \left(\frac{\partial^2 h}{\partial Q^2}\right)^2 dRdQ \qquad 58$$

$$k_R = \int_0^1 \int_0^1 \left(\frac{\partial h}{\partial R}\right)^2 dRdQ \qquad 59$$

$$k_Q = \int_0^1 \int_0^1 \left(\frac{\partial h}{\partial Q}\right)^2 dRdQ \qquad 60$$

Differentiating Equation 50 with respect to A_1 and simplifying the outcome gives:

$$\frac{N_x a^2}{D^*} = 6(1-2\mu)\left(\frac{a}{t}\right)^2 \left(\left[1+\left(\frac{k_{12}k_{23}-k_{13}k_{22}}{k_{12}k_{12}-k_{11}k_{22}}\right)\right] + \frac{1}{\beta^2}.\left[1+\left(\frac{k_{12}k_{13}-k_{11}k_{23}}{k_{12}k_{12}-k_{11}k_{22}}\right)\right].\frac{k_Q}{k_R}\right) 61$$

This gives:

$$\frac{N_x a^2}{Et^3} = \frac{(1+\mu)}{2}\left(\frac{a}{t}\right)^2 \left(\left[1+\left(\frac{k_{12}k_{23}-k_{13}k_{22}}{k_{12}k_{12}-k_{11}k_{22}}\right)\right] + \frac{1}{\beta^2}.\left[1+\left(\frac{k_{12}k_{13}-k_{11}k_{23}}{k_{12}k_{12}-k_{11}k_{22}}\right)\right].\frac{k_Q}{k_R}\right) \qquad 62$$

III. Numerical Analysis

The numerical buckling analysis of thick plate will be performed in this section, to obtain the value of the critical buckling load at various aspect ratios. A clamped rectangular plate is subjected to uniformly distributed compressive load. A fourth order polynomial displacement function as was derived in the previous section will be used to for the analysis CCCC rectangular plate.

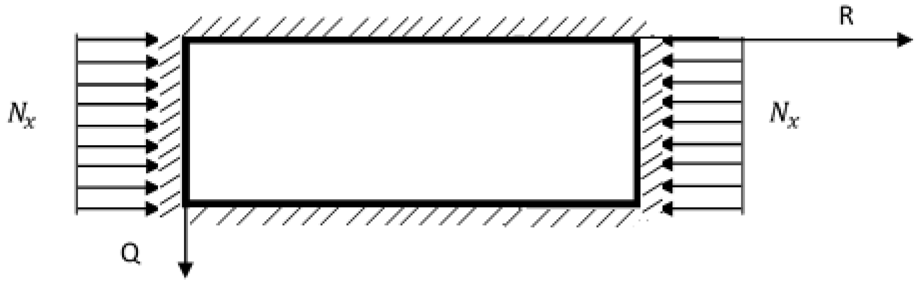

Figure 3: CCCC Rectangular Plate subjected to uniaxial compressive load

Simplifying Equation 44 gives:

$$w_{(x,y)} = (a_0 + a_1R + a_2R^2 + a_3R^3 + a_4R^4) \times (b_0 + b_1Q + b_2Q^2 + b_3Q^3 + b_4Q^4) \qquad 63$$

The boundary conditions of the plate in figure 3 are as follows:

At $R = Q = 0;\ w = 0$ 64

At At $R = Q = 0;\ \frac{dw}{dR} = \frac{dw}{dQ} = 0$ 65

At $R = Q = 1;\ w = 0$ 66

At $R = Q = 1; \frac{dw}{dR} = \frac{dw}{dQ} = 0$ 67

Substituting Equations (64 to 67) into Equation (63) and solving gives the following constants:

$a_0 = 0;\ a_1 = 0;\ a_2 = a_4;\ a_3 = -2a_4b_3$ 68

$b_0 = 0;\ b_1 = 0;\ b_2 = b_4;\ b_3 = -2b_4b_3$ 69

Substituting the constants of Equation (68) and (69) into Equation (63) gives;

$w = (a_4R^2 - 2a_4R^3 + a_4R^4) \times (b_4Q^2 - 2b_4Q^3 + b_4Q^4)$ 70

Simplifying Equation (70) which satisfying the boundary conditions of Equation (64 to 67) gave;

$w = a_4 \times b_4(R^2 - 2R^3 + R^4) \times (Q^2 - 2Q^3 + Q^4)$ 71

Recall from Equation 45, that;

$w = A_1h$

Let the amplitude,

$A_1 = a_4 \times b_4$ 72

And;

$h = (R^2 - 2R^3 + R^4) \times (Q^2 - 2Q^3 + Q^4)$ 74

Thus, the polynomial deflection functions after satisfying the boundary conditions is:

$w = (R^2 - 2R^3 + R^4) \times (Q^2 - 2Q^3 + Q^4).A_1$ 75

In the order hand, a trigonometric displacement function for the analysis CCCC plate derived according to author in [8] is given as presented in Equation (76).

$$w = (a_0 + \ a_1 R + a_2 \cos g_1 R + a_3 \sin g_1 R) \times (b_0 + \ b_1 Q + b_2 \cos g_2 Q + b_3 \sin g_2 Q) \qquad 76$$

The trigonometric displacement $w\ (x, y)$functions that satisfy the boundary conditions for all edges clamped rectangular plate boundary conditions are determined as follows:

Substituting Equation 64 to 67 into the derivatives of w and solving gave the characteristic equation as:

$$2Cos\ g_1 + g_1\ Sing_1 - 2 = 0 \qquad 77$$

The value of g_1 that satisfies Equation 77 is:

$$g_1 = 2m\pi\ [where\ m = 1, 2, 3 \ldots] \qquad 78$$

Substituting Equation 78 into the derivatives of wand satisfying the boundary conditions of Equation 64 to 67gives the following constants;

$$a_1 = a_3 = \ b_1 = b_3 = 0;\ a_0 = -a_2; b_0 = -b_2 = 0 \qquad 79$$

Substituting the constants of Equation 78 and 79 into Equation 76 gave;

$$w = a_0(1 - \ Cos2m\pi R) \times b_0(1 - \ Cos2m\pi Q) \qquad 80$$

Similarly;

$$w = a_2(\ Cos2m\pi R - 1) \times b_2(Cos2m\pi Q - 1) \qquad 81$$

Recall from Equation 45, that;

$$w = A_1 h$$

Let $m = 1$

Therefore:

$$w \ = a_2 \times b_2(\ Cos2\pi R - 1).(Cos2\pi Q - 1) \qquad 82$$

Let the amplitude,

$$A_1 = a_2 \times b_2 \qquad 83$$

And;

$$h = (Cos2\pi R - 1).(Cos2\pi Q - 1) \qquad 84$$

Thus, the trigonometric deflection functions after satisfying the boundary conditions is:

$$w = A_1(\ Cos2\pi R - 1).(Cos2\pi Q - 1) \qquad 85$$

IV. Results and Discussions

The result of stiffness coefficients for deflection of rectangular thick plate analysis subjected to the CCCC boundary condition was obtained using the polynomial and trigonometric shape function as obtained in Equation 75 and 85, their corresponding stiffness values are presented in Table 1. The proposed Poisson's ratio of the plate is 0.25.

Table 1: The polynomial and trigonometric stiffness coefficients of deflection function of the CCCC plate

Displacement Shape Function	k_{RR}	k_{RQ}	k_{QQ}	k_R	k_Q
Polynomial	0.00127	0.00036	0.00126	0.00003	0.00003
Trigonometric	1168.91	389.636	1168.91	29.6088	29.6088

The critical buckling load formulae $\left(\frac{N_x a^2}{\pi^2 D} \text{and} \frac{a^2 N_x}{Et^3}\right)$ were determined by applying the expression as obtained in Equation 61 and 62 respectively. Table 2 and 3 contains the result of the non-dimensional values of the critical buckling load $\left(\frac{N_x a^2}{\pi^2 D}\right)$ for an isotropic rectangular thick plate elastically restrained at the four edges (CCCC) under uniaxial compressive load at varying aspect ratio. Table 4 and 5 contains the result of the non-dimensional values of the critical buckling load $\left(\frac{a^2 N_x}{Et^3}\right)$ for an isotropic rectangular thick plate elastically restrained at the four edges (CCCC) under uniaxial compressive load at varying aspect ratio. Table 6 and Figure 4, 5, 6 and 7 presents the summary of the comparison between the present study using polynomial and that of trigonometric shape function. Figure 8 and 9 presents the CPT result comparison with Ibeabuchi *et al.*, 2020 and Iyangar, 1988.

For the non-dimensional values obtained in Table 2, 3, 4 and 5, it shows that the values of critical buckling load increase as the span- thickness ratio increases. This reveals that as the in-plane load on the plate increase and approaches the critical buckling, the failure in a plate structure is a bound to occur. This means that a decrease in plate thickness increases the chance of failure in a plate structure. Hence, failure tendency in the plate structure can be mitigated by increasing its thickness.

Critical look at Table 2 to 10, it is seen that an increase in the value of the length-breadth ratio ($\beta =$ 1.0, 1.5, 2.0, 2.5, 3.0, 3.5, 4.0, 4.5 and 5.0 decreases the value of the critical buckling load Nx. This means that an increase in plate width increases the chance of failure in a plate structure.

In summary, Table 2 to 5 and figure 4 to 7 presented here, it is observed that as the in-plane load which will cause the plate to fail by compression increases from zero to critical buckling load (N_{xcr}), the buckling of the plate exceed specified elastic limit thereby causing failure in the plate structure. This means that, the load that causes the plate to deform also causes the plate material to buckle simultaneously.

Table 2: Non-dimensional Critical Buckling Load $\frac{N_x a^2}{\pi^2 D}$ on the CCCC Rectangular Plate Using Polynomial Function

	$N_{xcr} = \frac{N_x a^2}{\pi^2 D}$								
$\propto = \frac{a}{t}$	$\beta = 1.0$	$\beta = 1.5$	$\beta = 2.0$	$\beta = 2.5$	$\beta = 3.0$	$\beta = 3.5$	$\beta = 4.0$	$\beta = 4.5$	$\beta = 5.0$
4	6.67690	4.1471	3.4802	3.2277	3.1083	3.0429	3.0033	2.9775	2.9597
5	7.99385	4.8477	4.0569	3.7627	3.6242	3.5486	3.5027	3.4727	3.4521
10	10.8463	6.2669	5.2172	4.8367	4.6589	4.5617	4.5027	4.4641	4.4374
15	11.6137	6.6281	5.5105	5.1077	4.9197	4.8169	4.7544	4.7136	4.6853
20	11.9086	6.7647	5.6213	5.2100	5.0180	4.9131	4.8493	4.8076	4.7787
30	12.1286	6.8658	5.7032	5.2856	5.0908	4.9842	4.9195	4.8771	4.8478
40	12.2075	6.9019	5.7325	5.3126	5.1167	5.0096	4.9445	4.9019	4.8725
50	12.2444	6.9188	5.7461	5.3252	5.1288	5.0215	4.9562	4.9135	4.8839
60	12.2645	6.928	5.7536	5.3320	5.1354	5.0279	4.9626	4.9198	4.8902
70	12.2767	6.9335	5.7581	5.3362	5.1394	5.0318	4.9664	4.9236	4.8940
80	12.2846	6.9371	5.7610	5.3389	5.1420	5.0344	4.9689	4.9261	4.8965
90	12.2900	6.9396	5.7630	5.3407	5.1438	5.0361	4.9706	4.9278	4.8981
100	12.2939	6.9414	5.7644	5.3420	5.1451	5.0373	4.9719	4.9290	4.8994
1000	12.3104	6.9489	5.7705	5.3476	5.1504	5.0426	4.9771	4.9341	4.9045
1500	12.3105	6.9489	5.7705	5.3477	5.1505	5.0426	4.9771	4.9342	4.9045

Table 3: Non-dimensional Critical Buckling Load $\frac{N_x a^2}{Et^3}$on the CCCC Rectangular Plate Using Polynomial Function

	$N_{xcr} = \frac{N_x a^2}{Et^3}$								
$\propto = \frac{a}{t}$	$\beta = 1.0$	$\beta = 1.5$	$\beta = 2.0$	$\beta = 2.5$	$\beta = 3.0$	$\beta = 3.5$	$\beta = 4.0$	$\beta = 4.5$	$\beta = 5.0$
4	5.85760	3.6383	3.0531	2.8316	2.7269	2.6696	2.6348	2.6122	2.5966
5	7.01300	4.2528	3.5591	3.3010	3.1795	3.1131	3.0729	3.0466	3.0285
10	9.51540	5.4980	4.5770	4.2432	4.0873	4.0020	3.9502	3.9164	3.8930
15	10.1887	5.8148	4.8344	4.4810	4.3160	4.2258	4.1710	4.1352	4.1104
20	10.4474	5.9346	4.9316	4.5707	4.4023	4.3103	4.2543	4.2177	4.1924
30	10.6404	6.0234	5.0034	4.6370	4.4661	4.3727	4.3159	4.2787	4.2530
40	10.7096	6.0550	5.0291	4.6607	4.4889	4.3949	4.3378	4.3005	4.2746
50	10.7420	6.0698	5.0411	4.6718	4.4995	4.4053	4.3481	4.3106	4.2847
60	10.7597	6.0779	5.0476	4.6778	4.5053	4.4110	4.3537	4.3161	4.2902
70	10.7703	6.0828	5.0515	4.6814	4.5088	4.4144	4.3570	4.3195	4.2935
80	10.7773	6.0859	5.0541	4.6838	4.5111	4.4166	4.3592	4.3216	4.2957
90	10.7820	6.0881	5.0559	4.6854	4.5126	4.4182	4.3607	4.3231	4.2971
100	10.7854	6.0897	5.0571	4.6866	4.5138	4.4192	4.3618	4.3242	4.2982
1000	10.7999	6.0962	5.0624	4.6915	4.5185	4.4239	4.3664	4.3287	4.3027
1500	10.7999	6.0963	5.0625	4.6915	4.5185	4.4239	4.3664	4.3287	4.3027

Table 4: Non-dimensional Critical Buckling Load $\frac{N_x a^2}{\pi^2 D}$ on the CCCC Rectangular Plate Using Trigonometric Function

	$N_{xcr} = \frac{N_x a^2}{\pi^2 D}$								
$\propto= \frac{a}{t}$	$\beta = 1.0$	$\beta = 1.5$	$\beta = 2.0$	$\beta = 2.5$	$\beta = 3.0$	$\beta = 3.5$	$\beta = 4.0$	$\beta = 4.5$	$\beta = 5.0$
4	6.5845	4.0716	3.3996	3.1408	3.0166	2.9478	2.9057	2.8780	2.8589
5	7.8617	4.7424	3.9446	3.6422	3.4977	3.4178	3.3689	3.3368	3.3145
10	10.605	6.0850	5.0242	4.6320	4.446	4.3432	4.2802	4.2388	4.2101
15	11.337	6.4231	5.2936	4.8783	4.6815	4.5728	4.5062	4.4624	4.4320
20	11.618	6.5506	5.3950	4.9708	4.7700	4.6591	4.5911	4.5464	4.5153
30	11.827	6.6448	5.4698	5.0392	4.8353	4.7227	4.6537	4.6083	4.5768
40	11.902	6.6785	5.4965	5.0635	4.8586	4.7454	4.6761	4.6304	4.5987
50	11.937	6.6941	5.5090	5.0749	4.8695	4.7560	4.6865	4.6407	4.6089
60	11.956	6.7027	5.5158	5.0811	4.8754	4.7617	4.6921	4.6463	4.6145
70	11.968	6.7079	5.5199	5.0848	4.879	4.7652	4.6956	4.6497	4.6179
80	11.975	6.7112	5.5225	5.0872	4.8813	4.7675	4.6978	4.6519	4.6200
90	11.981	6.7135	5.5244	5.0889	4.8829	4.7690	4.6993	4.6534	4.6215
100	11.984	6.7152	5.5257	5.0901	4.884	4.7701	4.7004	4.6545	4.6226
1000	12.000	6.7222	5.5312	5.0951	4.8888	4.7748	4.7050	4.6591	4.6272
1500	12.000	6.7222	5.5312	5.0952	4.8889	4.7749	4.7051	4.6591	4.6272

Table 5: Non-dimensional Critical Buckling Load $\frac{N_x a^2}{Et^3}$on the CCCC Rectangular Plate Using Trigonometric Function

	$N_{xcr} = \frac{N_x a^2}{Et^3}$								
$\propto= \frac{a}{t}$	$\beta = 1.0$	$\beta = 1.5$	$\beta = 2.0$	$\beta = 2.5$	$\beta = 3.0$	$\beta = 3.5$	$\beta = 4.0$	$\beta = 4.5$	$\beta = 5.0$
4	5.7766	3.5720	2.9824	2.7554	2.6465	2.5861	2.5492	2.5249	2.5081
5	6.8971	4.1605	3.4606	3.1953	3.0685	2.9984	2.9556	2.9274	2.9078
10	9.3033	5.3384	4.4077	4.0636	3.9004	3.8102	3.7550	3.7187	3.6935
15	9.9459	5.6349	4.6441	4.2797	4.1071	4.0117	3.9533	3.9149	3.8882
20	10.192	5.7468	4.7330	4.3609	4.1847	4.0874	4.0278	3.9886	3.9613
30	10.376	5.8295	4.7987	4.4208	4.2420	4.1432	4.0827	4.0429	4.0152
40	10.442	5.8590	4.8221	4.4422	4.2625	4.1631	4.1023	4.0623	4.0344
50	10.472	5.8728	4.8330	4.4522	4.2720	4.1724	4.1114	4.0713	4.0434
60	10.489	5.8803	4.8390	4.4576	4.2772	4.1775	4.1164	4.0762	4.0483
70	10.499	5.8848	4.8426	4.4609	4.2803	4.1805	4.1194	4.0792	4.0512
80	10.506	5.8877	4.8449	4.4630	4.2823	4.1825	4.1214	4.0811	4.0532
90	10.511	5.8898	4.8465	4.4645	4.2837	4.1839	4.1227	4.0824	4.0545
100	10.514	5.8912	4.8477	4.4655	4.2847	4.1848	4.1237	4.0834	4.0554
1000	10.527	5.8973	4.8525	4.4700	4.2890	4.1890	4.1277	4.0874	4.0594
1500	10.528	5.8974	4.8525	4.4700	4.2890	4.1890	4.1277	4.0874	4.0594

In comparison, it can be seen in table 2 to 5 and figure 4 to 9 that the value of the critical buckling load using polynomial is higher than that of trigonometric functions. This is quite expected because the trigonometric function gives higher value of stiffness coefficient than polynomial, and therefore considers safer to use in the thick plate analysis. Comparing the buckling coefficients *K* of the Ibeabuchi *et al*., 2020 which made use of the polynomial function of the work principle with K_T from an analytical solution that used a trigonometric function, shows good agreement (average percentage difference is 0.*446*%) with but varied widely with the present study.

The percentage difference of critical buckling load between the present study using polynomial, and that of trigonometric function for an isotropic rectangular thick plate elastically restrained at the four edges (CCCC) under uniaxial compressive load at varying aspect ratio is presented in Table 6. The result showed that the lowest average percentage difference is 1.3841 which occur at ratio and the highest average percentage difference is 5.6543 which occur at a ratio. This means that as the aspect ratio (span to thickness ratio and length to width ratio) increases, the value of the buckling load of the plate using the two approaches (polynomial and trigonometric) widens.

The summary result of the comparison made as presented in Table 6 and Figure 4 to 9, shows that the present study predicts slightly higher values for all aspect ratios. This proves some level safety and reliability of this method as it will not put the structure into danger. The total average percentage difference between the present study using the polynomial shear deformation theory and that of trigonometric is 4.3%. This shows that at the 92 % confidence level both methods from the present study are the same. This value has been less than 5% is sufficient in the statistical analysis showed that the present method can be used with confidence for buckling analysis of CCCC thick plate.

Table 6: Percentage difference of Buckling Load on the CCCC Rectangular Plate between Polynomial and trigonometric Approach

	Average Percentage Difference %								
$\propto = \frac{a}{t}$	$\beta = 1.0$	$\beta = 1.5$	$\beta = 2.0$	$\beta = 2.5$	$\beta = 3.0$	$\beta = 3.5$	$\beta = 4.0$	$\beta = 4.5$	$\beta = 5.0$
4	1.3841	1.8212	2.3163	2.6916	2.9498	3.1270	3.2514	3.3411	3.4076
5	1.6526	2.1720	2.7697	3.2026	3.4909	3.6846	3.8187	3.9146	3.9851
10	2.2291	2.9027	3.6993	4.2326	4.5707	4.7911	4.9408	5.0463	5.1233
15	2.3831	3.0928	3.9365	4.4921	4.8409	5.0670	5.2199	5.3275	5.4058
20	2.4421	3.1650	4.0262	4.5899	4.9426	5.1707	5.3248	5.4331	5.5118
30	2.4861	3.2186	4.0925	4.6622	5.0177	5.2472	5.4022	5.5110	5.5901
40	2.5019	3.2378	4.1163	4.6880	5.0444	5.2745	5.4298	5.5388	5.6180
50	2.5093	3.2467	4.1270	4.7000	5.0569	5.2873	5.4426	5.5517	5.6310
60	2.5133	3.2516	4.1333	4.7066	5.0637	5.2942	5.4496	5.5588	5.6381
70	2.5157	3.2545	4.1370	4.7105	5.0678	5.2984	5.4539	5.5630	5.6424
80	2.5173	3.2565	4.1393	4.7131	5.0705	5.3011	5.4566	5.5658	5.6452
90	2.5184	3.2578	4.1410	4.7149	5.0723	5.3030	5.4585	5.5677	5.6471
100	2.5192	3.2587	4.1421	4.7162	5.0737	5.3043	5.4599	5.5691	5.6485
1000	2.5224	3.2627	4.1471	4.7215	5.0792	5.3100	5.4656	5.5748	5.6542
1500	2.5225	3.2627	4.1471	4.7215	5.0792	5.3100	5.46561	5.5749	5.6543
Average % difference	2.35	3.04	3.87	4.4176	4.76	4.98	5.14	5.24	5.32
Total Average % difference	4.3								

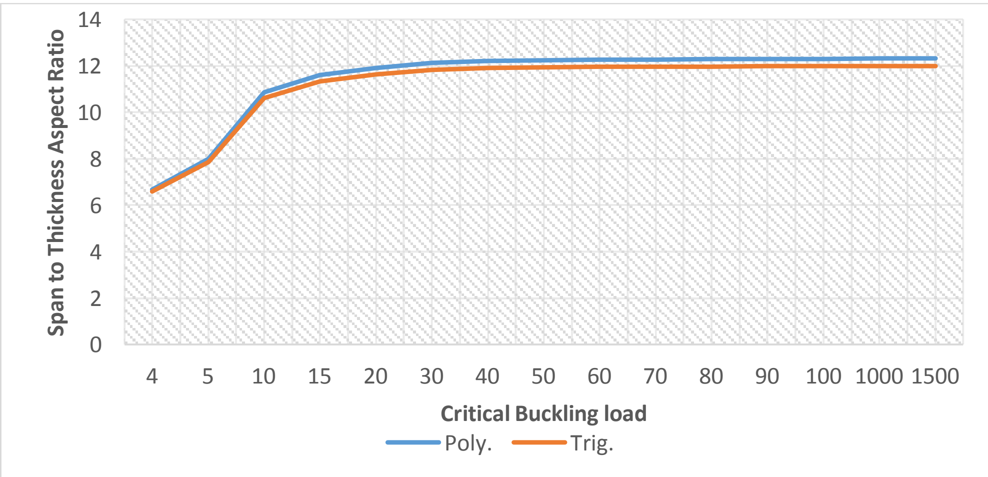

Figure 4: Graph of Critical buckling load$\left(\frac{N_x a^2}{\pi^2 D}\right)$ versus aspect ratio of a square rectangular plate

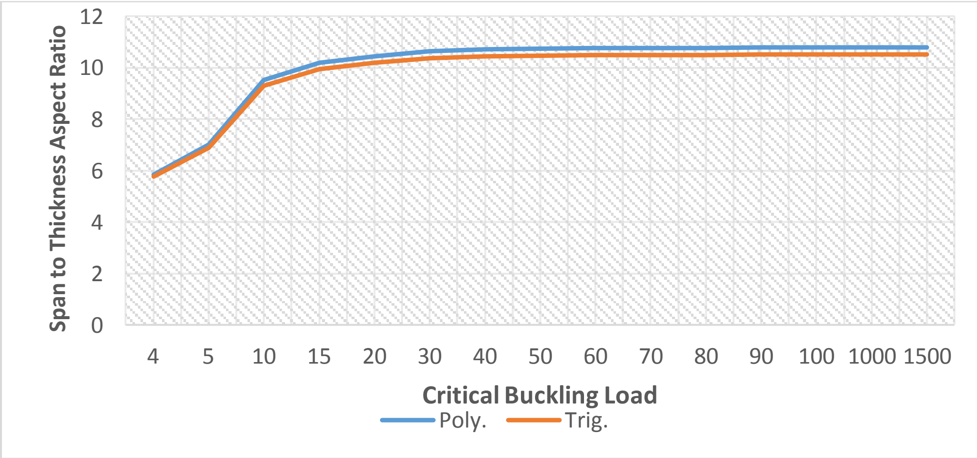

Figure 5: Graph of Critical buckling load $\left(\frac{N_x a^2}{Et^3}\right)$versus aspect ratio of a square rectangular plate

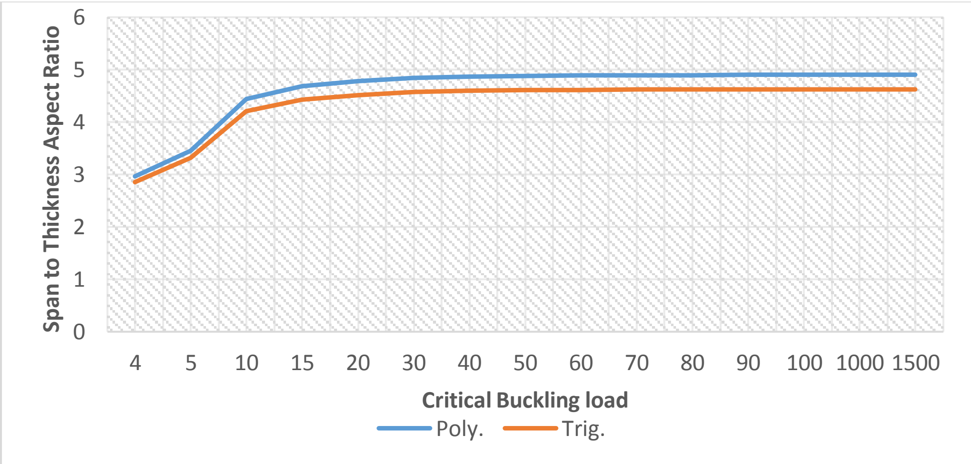

Figure 6: Graph of Critical buckling load$\left(\frac{N_x a^2}{\pi^2 D}\right)$ versus aspect ratio of a rectangular plate with length to width ratio of 5.

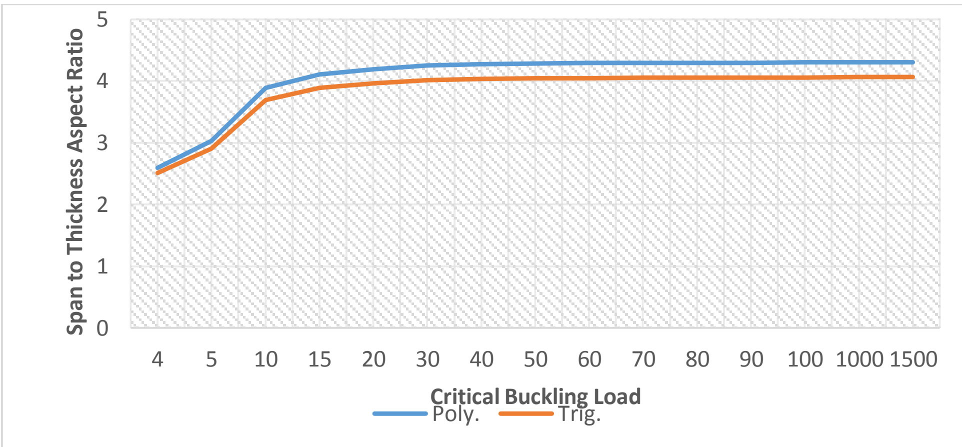

Figure 7: Graph of Critical buckling load $\left(\frac{N_x a^2}{Et^3}\right)$versus aspect ratio of a rectangular plate with length to width ratio of 5.

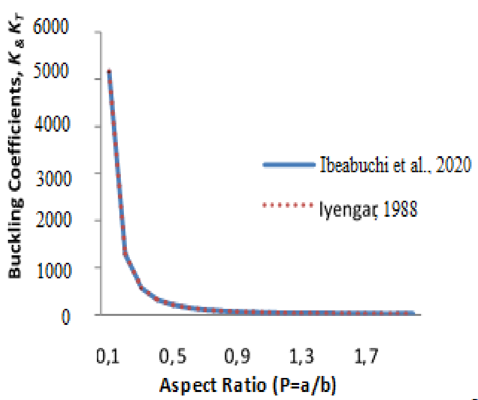

Fig.8: Buckling coefficient vs aspect ratio stiffened plate for α =10, β= 0.1

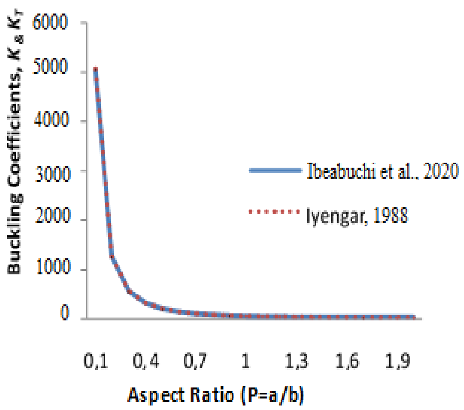

Fig.9: Buckling coefficient vs aspect ratio stiffened plate for α =5, β =0.05

V. Conclusion ad Recommendation

From the result obtained in this study, it is observed that CPT and gives reliable results in thin plates, but over-predicts buckling loads in relatively thick plates. Also, the RPT gives is an approximate relation for buckling analysis of thick plate, whereas 3-D theory yields an exact solution. This proved that the displacement functions (polynomial and trigonometric) developed in this work are recommended for the thick plate analysis.

Data Availability Statement: All data, models, or code that support the findings of this study are available from the corresponding author upon reasonable request.

References

[1]. Timoshenko S.P. and Gere J.M. (1961): *Theory of Elastic Stability*. – New York: McGraw-Hill.

[2]. Zhang K. and Lin T.R. (2019): *Analytical study of vibration response of a beam stiffened Mindlin plate*. − Applied Acoustics, vol.155, pp.32-43.

[3]. Timoshenko, S.P. and Woinowsky-Krieger.(1987). Theory of Plates and Shells. *Second Edition McGraw Hill Publishing Company, pp. 2*.

[4]. Ike, C.C. (2017). Equilibrium Approach in the Derivation of Differential Equations for Homogeneous Isotropic Mindlin Plates.*Nigerian Journal of Technology (NIJOTECH), 36*(2):346-350. http://dx.doi.org/10.4314/njt.v36i2.4

[5]. Reddy, J.N. (2007). Theory and Analysis of Elastic Plates and Shells. *Second Edition CRC Press, Taylor and Francis Group USA*.

[6]. Iyengar, N.G.R. (1988). Structural Stability of Columns and Plates.*Chichester: Ellis Horwood*.

[7]. Zenkour A. M. (2003) Exact Mixed-Classical Solutions for the Bending Analysis of Shear Deformable Rectangular Plates, Applied Mathematical Modelling, 27(7): 515-534.

[8]. Onyeka, F.C., Osegbowa, D. and Arinze, E.E., (2020). Application of a New Refined Shear Deformation Theory for the Analysis of ThickRectangular Plates. *Nigerian Research Journal of Engineering and Environmental Sciences*, *5*(2): 901-917.

[9]. Ibearugbulem, O.M, Ibeabuchi, V.T. and Njoku, K.O. (2014): *Buckling analysis of SSSS stiffened rectangular isotropic plates using work principle approach*. – International Journal of Innovative Research & Development, vol.3, No.11, pp.169-176.

[10]. Ibeabuchi, V.T., Ibearugbulem, O.M., Ezeah, C. and Ugwu, O.O. (2020). Elastic Buckling Analysis of Uniaxially Compressed CCCC Stiffened Isotropic Plates. *Int. J. of Applied Mechanics and Engineering*, *25*(4): 84-95. DOI: 10.2478/ijame-2020-0051.

[11]. Shufrin and Eisenberger, M (2005). Stability and vibration of shear deformable plates - First order and higher order analyses. *International Journal of Solids and Structures*, *42*(3-4): 1225–1251.

[12]. Onyeka, F.C., Okafor, F.O. and Onah H.N. (2021). Application of a New Trigonometric Theory in the Buckling Analysis of Three-Dimensional Thick Plate. *International Journal of Emerging Technologies*, *12*(1): 228–240.

Onyeka, F. C, et. al. "Buckling Solution of a Three-Dimensional Clamped Rectangular Thick Plate Using Direct Variational Method." *IOSR Journal of Mechanical and Civil Engineering (IOSR-JMCE)*, 18(3), 2021, pp. 10-22.